

RESEARCH

Open Access



# Liver macrophage-derived exosomal miRNA-342-3p promotes liver fibrosis by inhibiting HPCAL1 in stellate cells

Wenshuai Li<sup>1†</sup>, Lirong Chen<sup>1†</sup>, Qi Zhou<sup>1†</sup>, Tiansheng Huang<sup>2</sup>, Wanwei Zheng<sup>1</sup>, Feifei Luo<sup>1</sup>, Zhong Guang Luo<sup>1\*</sup>, Jun Zhang<sup>1\*</sup> and Jie Liu<sup>1\*</sup>

## Abstract

**Background** The progression of liver fibrosis involves complex interactions between hepatic stellate cells (HSCs) and multiple immune cells in the liver, including macrophages. However, the mechanism of exosomes in the crosstalk between liver macrophages and HSCs remains unclear.

**Method** Exosomes were extracted from primary mouse macrophages and cultured with HSCs, and the differential expression of microRNAs was evaluated using high-throughput sequencing technology. The functions of miR-342-3p in exosomes were verified by qPCR and luciferase reporter gene experiments with HSCs. The function of the target gene Hippocalcin-like protein 1 (HPCAL1) in HSCs was verified by Western blotting, qPCR, cellular immunofluorescence and co-IP in vivo and in vitro.

**Results** We demonstrated that exosomal microRNA-342-3p derived from primary liver macrophages could activate HSCs by inhibiting the expression of HPCAL1 in HSCs. HPCAL1, which is a fibrogenesis suppressor, could inhibit TGF- $\beta$  signaling in HSCs by regulating the ubiquitination of Smad2 through direct interactions with its EF-hand 4 domain.

**Conclusion** This study reveals a previously unidentified profibrotic mechanism of crosstalk between macrophages and HSCs in the liver and suggests an attractive novel therapeutic strategy for treating fibroproliferative liver diseases.

**Keywords** Liver fibrosis, Liver macrophage, Exosome, Hepatic stellate cells, MiRNA-342-3p

<sup>†</sup>Wenshuai Li, Lirong Chen and Qi Zhou have contributed equally to this work.

\*Correspondence:

Zhong Guang Luo

luozg8@126.com

Jun Zhang

archsteed@163.com

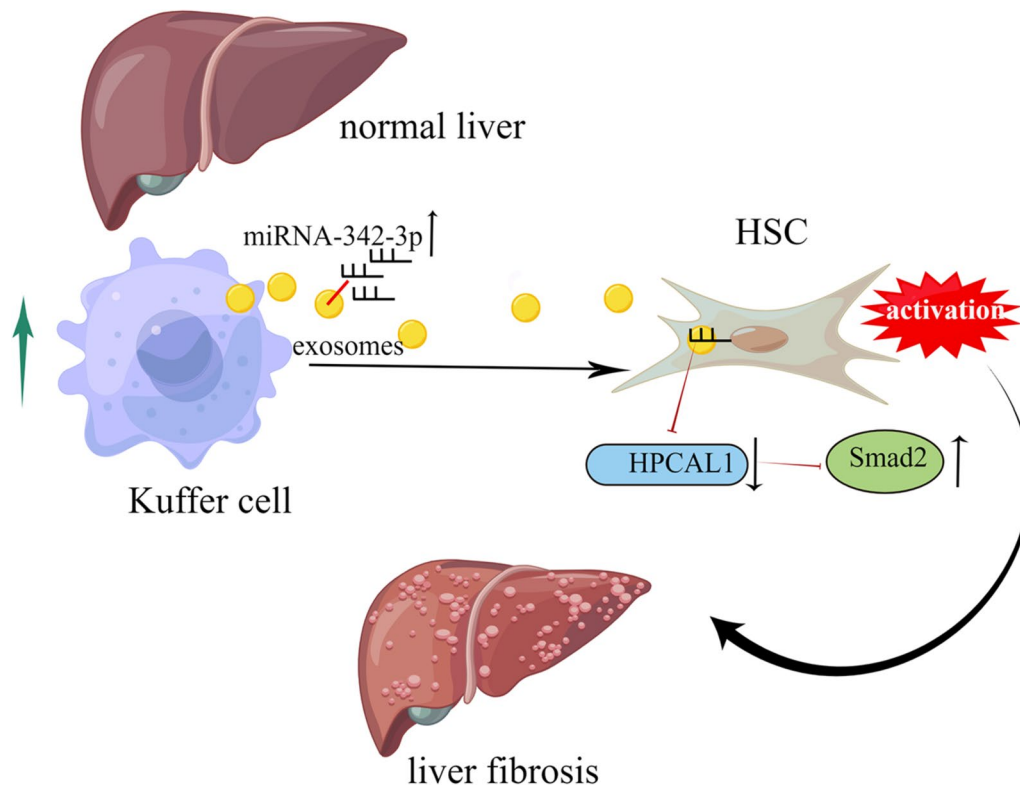
Jie Liu

jieliu@fudan.edu.cn

Full list of author information is available at the end of the article



## Graphical Abstract



## Introduction

The dynamic process of liver fibrosis, caused by a variety of causes such as viral infection, alcohol abuse, and aberrant energy metabolism, is a chronic liver damage. The liver condition followed by untreated, liver fibrosis ultimately deteriorates into cirrhosis or hepatocellular carcinoma (HCC) with unfavorable prognosis. Therefore, there is a pressing requirement to reverse these end-stage liver diseases. However, clinically targeted drugs for liver fibrosis are not effective [1–4].

The intricate liver environment is greatly dependent on the communication between its various cell types. A major histological element of liver fibrosis is the production of fibrillar collagens and extracellular matrix (ECM) by activated hepatic stellate cells (HSCs). HSCs activation can be facilitated by different cell types in the liver, including infiltrating immune cells. In particular, liver macrophages are critical for triggering and sustaining HSC activation by generating fibrogenic cytokines, such as TGF- $\beta$ , CCL2, CCL5, and IL-1 $\beta$  [5–8]. Exosomes, which mediate intercellular communication, are released by stressed parenchymal cells and can transmit stress signals to neighboring immune cells, including

macrophages [2, 8]. For example, studies have shown that hepatocyte-derived extracellular vesicles can accelerate liver fibrosis by inducing the expression of proinflammatory cytokines such as IL-1 $\beta$  and IL-6 in mouse bone marrow-derived macrophages (BMDMs) [10]. It was shown that exosomes derived from lipopolysaccharide (LPS)-treated macrophages have increased levels of miR-500, and exosomes containing miR-500 promoted HSCs proliferation and activation by suppressing MFN2 [11].

We demonstrated in this study that primary hepatic macrophages could influence the activation of stellate cells by releasing exosomes containing microRNA-342-3p, which could impede the expression of Hippocalcin-like protein 1 (HPCAL1), thus impacting the activation of stellate cells. HPCAL1, also known as visinin-like protein 3 (VILIP-3), is a neuronal calcium sensor protein belonging to the VILIP superfamily. HPCAL1 plays a significant role in tumor formation and development [12–17]. Our previous study showed that HPCAL1 was a novel tumor suppressor that regulated HCC cell cycle progression and might be a diagnostic and prognostic factor for HCC [16]. However, the biological functions of HPCAL1 in liver fibrosis, which is a

precancerous lesion of HCC, remain largely unclear. In this context, our study uncovered a previously unrecognized profibrotic mechanism in the liver involving the interaction between macrophages and HSCs. We also identified a novel and crucial role of HPCAL1 in HSC activation, offering new insights into the pathogenesis of liver fibrosis. These findings highlight HPCAL1 as a potential therapeutic target for treating fibroproliferative liver diseases.

## Materials and methods

### Animal model

The 8-week-old male C57BL/6 J mice underwent an intraperitoneal injection of carbon tetrachloride (CCl<sub>4</sub>, 10%) in olive oil (0.01 ml/g/mouse) twice weekly, resulting in liver fibrosis [18]. The same amount of olive oil was injected intraperitoneally into the mice from control group. 20 mice were randomly divided into four groups as follows: olive oil (NC; n=5), CCl<sub>4</sub> induced fibrosis model (CCl<sub>4</sub>; n=5), CCl<sub>4</sub> combined with the injection of LV-Con (LV-Con + CCl<sub>4</sub>; n=5), and CCl<sub>4</sub> combined with the injection of LV-HPCAL1 (LV-HPCAL1 + CCl<sub>4</sub>; n=5). LV-Con and LV-HPCAL1 were injected once at  $1 \times 10^8$  virus particles/50  $\mu$ l per mouse three days before the first CCl<sub>4</sub> injection via the tail vein. After 8 weeks, the animals were sacrificed, and their liver tissue was harvested for fixation with 10% formalin and cryopreservation with liquid nitrogen.

### Western blotting

Using a bicinchoninic acid protein assay kit (Beyotime Institute of Biotechnology, Shanghai, China), RIPA buffer was employed to lyse the liver tissue, and the total protein was then quantified. The membranes were incubated overnight with primary antibodies at 4 °C. After being cultured with primary antibodies, and horseradish peroxidase-conjugated secondary antibodies (diluted at 1:2,000) were then incubated for 1 h. An improved chemiluminescence system was employed to detect the signals, and images were captured by a gel imaging analysis system (TANON 4100, TANON Science and Technology Co., Shanghai, China). Primary antibodies information: Anti-HPCAL1 (1:500 dilution, Proteintech, CN: 10989-1-AP), Anti- $\alpha$ -SMA (1:1000 dilution, Abcam, CN: 32575), Anti-Coll1a1 (Human/Mouse) (1:1000 dilution, Abcam, CN: 138492/2128), Anti-GAPDH (1:2000 dilution, Abcam, CN: 181603), Anti-SMAD2/SMAD3 (1:1000 dilution, CST, CN: 5339/9523), Anti-p-SMAD2/SMAD3 (1:500 dilution, CST, CN: 3108/9520).

### RNA extraction and real-time PCR

The FastQuant RT Kit (Tiangen, China) was utilized to synthesize complementary DNA (cDNA) from total RNA

extracted from liver tissues, which was stored at  $-80$  °C and lysed with TRIzol reagent (Invitrogen) in accordance with the manufacturer's protocol. Subsequently, amplification with the Bio-Rad Real-Time PCR System was employed to calculate relative mRNA expression levels, using the  $2^{-\Delta\Delta CT}$  method.

### Immunohistochemistry

Histological slices were deparaffined in xylene and dehydrated with ethanol. Endogenous peroxidase was blocked by hydrogen peroxide for 15 min. Subsequently, a blocking solution of 5% bovine serum albumin (BSA) was applied to the sections for 20 min, and they were incubated with primary antibodies against  $\alpha$ -smooth muscle actin ( $\alpha$ -SMA, 1:200), collagen type I (collagen I, 1:200), and HPCAL1 (1:200) at 4 °C overnight. After being rinsed, the sections were incubated with biotinylated goat anti-rabbit immunoglobulins for 1 h. To observe the antibody-antigen complexes, the sections were treated with streptavidin and diaminobenzidine, which had been peroxidase-conjugated, then counterstained with Mayer's hematoxylin. The study methodologies conformed to the standards set by the Declaration of Helsinki.

### Immunofluorescence staining

After incubation for 12 h on 18-mm cover slips, LX-2 cells were fixed with a milliliter of 4% formaldehyde fixative solution for 15 min. Subsequently, the samples were incubated with primary antibodies against  $\alpha$ -SMA and collagen I at 4 °C in a humidified chamber overnight. Finally, the samples were incubated with a fluorescein-labeled secondary antibody (1:500 dilution in antibody dilution solution) in the dark for 1 h. At room temperature, 4,6-diamino-2-phenyl indole (DAPI) was used to stain the nuclei for 15 min. One drop of antifade medium was then used to mount the cells or slides, and the stained cells or slides were then viewed with a fluorescence microscope and the appropriate filters.

### Transient transfection

Biotend Company (Shanghai, China) synthesized all small interfering RNAs (siRNAs) and nonspecific control siRNAs, which were then transfected into cells with Lipofectamine 2000 transfection reagent (Invitrogen) in accordance with the manufacturer's instructions.

### Dual-luciferase reporter assay

Culturing 293 T cells in 24-well plates, transfection with pmirGLO-HPCAL1-WT or pmirGLO-HPCAL1-Mutant, as well as miR-342-3p mimics or NC mimics, was performed. After 48 h, the cells were harvested and transferred to 1.5 ml Eppendorf (EP) tubes. The Dual-Glo

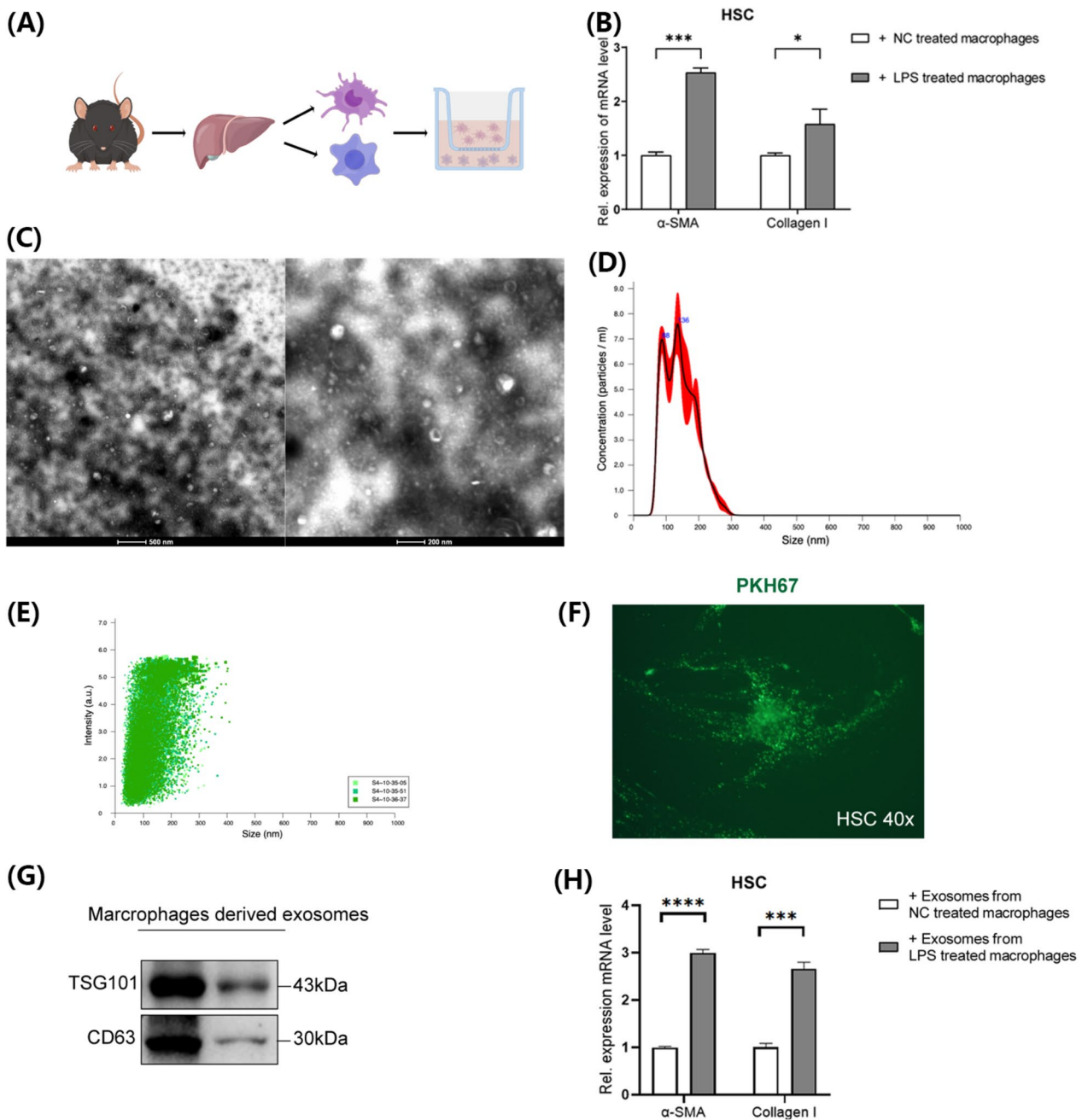


**Fig. 1** Macrophage-derived exosomes mediate the increase in HSC activation. **(A)** Primary liver macrophages and HSCs were isolated from the livers of C57Bl/6 mice and cocultured for 48 h in Transwell chambers. **(B)** Real-time qPCR analysis of α-SMA and collagen I in HSCs cocultured with control and LPS-treated liver macrophages for 48 h. Student’s t test was used for statistical analysis (\*P < 0.05, \*\*\*P < 0.001). **(C)** Electron microscopic images of exosomes secreted by liver macrophages. Scale bars: 500 μm and 200 μm. **(D, E)** Analysis of the NTA diameter **(D)** and density **(E)** of exosomes by the spin-out method. **(F)** Exosomes secreted by liver macrophages stained with PKH67 green fluorescence that were taken up by HSCs. **(G)** Western blot analysis to detect the marker proteins CD63 and TSG101 in exosomes secreted by liver macrophages. The gel images were cropped to show only relevant proteins. **(H)** Real-time qPCR analysis of α-SMA and collagen I in HSCs containing exosomes secreted by control and LPS-treated liver macrophages for 48 h. Student’s t test was used for statistical analysis (\*\*\*\*P < 0.0001)

Luciferase Assay System (Promega, Madison, WI) was employed in accordance with the manufacturer’s protocol.

**The culture and isolation of HSCs and liver macrophages** After anesthetizing the mice with Pentobarbitone, the abdominal cavity was opened to expose the hepatic portal

vein. Two venous indwelling needles were inserted into the inferior vena cava and the hepatic portal vein, both of which were then secured with surgical sutures and connected to the peristaltic pump of a perfusion device. The liver was then perfused with a preheated heparin-containing solution, followed by collagenase solution. After collecting and washing the liver tissue with PBS, a whole cell suspension was filtered and centrifuged. This suspension was then layered with Percoll solution and spun again to differentiate between liver macrophages (adherent cells) and HSCs (nonadherent cells). The supernatant was discarded and the precipitate was resuspended in medium, transferred to a T-25 culture bottle, and incubated in a 37 °C incubator for 60 min. Adherent liver macrophages were the cells, while HSCs were the nonadherent ones.

#### Exosome extraction

First, collect the cell culture supernatant and filter it through a 0.8 µm filter membrane. Add an equal volume of XBP and mix by inverting the tube 5 times. Then, transfer the mixture to an exoEasy spin column, centrifuge at 500 g for 1 min, and discard the flow-through. Add 10 mL of Buffer XWP to the spin column and centrifuge at 5000 g for 5 min, discarding the flow-through. Place the spin column into a new tube, add 400 µL to 1 mL of Buffer XE onto the spin column membrane, incubate at room temperature for 1 min, and centrifuge at 500 g for 5 min. Add the flow-through back onto the spin column membrane, incubate at room temperature for 1 min, and centrifuge at 5000 g for 5 min. The flow-through is the exosome, which can be used for identification or functional assays. Store at -80 °C. For detailed steps, refer to the QIAGEN 76064 exoEasy Maxi Kit protocol.

#### Immunoprecipitation

Cells were lysed using a cell lysis buffer (CST) supplemented with a complete protease inhibitor cocktail (Roche, Switzerland). Protein-G agarose beads (Invitrogen Life Technologies) were incubated overnight with either an anti-HPCAL1/SMAD2/FLAG antibody or a non-specific rabbit IgG antibody. The protein lysates were then added to the beads and incubated overnight. After incubation, the bead-protein mixture was placed on a magnetic rack (Biotool, cat. no. B23803) for a few seconds to separate the beads from the supernatant. The bead-bound complexes were washed several times with lysis buffer, and then subjected to Western blot analysis.

#### Statistical analysis

A comparison of normally distributed data between groups and paired data was conducted using ANOVA and Student's t test, with the mean ± SEM values reported and a P value of less than 0.05 being deemed statistically significant.

## Results

### Macrophage-derived exosomes mediate the increase in HSC activation

Primary liver macrophages and HSCs were isolated from C57BL/6 mouse livers and cocultured in the upper and lower chambers of transwell plates, respectively (Fig. 1A). α-SMA and collagen I are typical markers of HSC activation. The transcriptional levels of α-SMA and collagen I were elevated in the presence of LPS-treated macrophages (Fig. 1B). Thus, we hypothesized that the substances secreted by macrophages could upregulate HSC activation. Electron microscopy showed the presence of exosomes in the supernatant, and nanoparticle tracking analysis confirmed that these particles were vesicles

(See figure on next page.)

**Fig. 2** HSC activation was promoted by macrophage-derived exosomal miRNA-342-3p by inhibiting HPCAL1. **(A)** MicroRNA sequencing of exosomes secreted by primary hepatic macrophages from control C57Bl6 mice and C57Bl6 mice with CCl4-induced liver fibrosis. **(B)** MicroRNA sequencing of primary stellate cells from control C57Bl6 mice and C57Bl6 mice with CCl4-induced liver fibrosis. **(C)** The expression level of miRNA-342-3p in control primary liver macrophages (cell culture for 5 days after primary cell extraction), in control primary liver macrophages cultured for 14 days and in primary liver macrophages isolated from mice with CCl4-induced liver fibrosis. Student's t test was used for statistical analysis (\*\*\*\*P < 0.0001). **(D)** The expression level of miRNA-342-3p in exosomes secreted by control primary liver macrophages (cultured for 5 days after primary cell extraction), primary liver macrophages cultured for 14 days, and primary liver macrophages isolated from mice with CCl4-induced liver fibrosis. Student's t test was used for statistical analysis (\*\*P < 0.01, \*\*\*P < 0.001). **(E)** Exosomes secreted by control liver macrophages and liver macrophages overexpressing miRNA-342-3p were added to HSCs. Real-time qPCR analysis of the expression of miRNA-342-3p in HSCs. Student's t test was used for statistical analysis (\*\*\*P < 0.001). **(F)** 3'UTR binding site of miRNA-342-3p and HPCAL1. **(G)** Dual luciferase reporter assay showing that miR-342-3p directly binds to the 3'UTR of HPCAL1, suggesting that HPCAL1 is a direct target of miR-342-3p. Student's t test was used for statistical analysis (\*\*P < 0.01). **(H, I)** The mRNA and protein expression of α-SMA, Collagen I and HPCAL1 in primary HSCs overexpressing miRNA-342-3p. Student's t test was used for statistical analysis (\*\*P < 0.01). **(J)** The mRNA expression levels of α-SMA, Collagen I and HPCAL1 in LX2 cells overexpressing miRNA-342-3p. Student's t test was used for statistical analysis (\*P < 0.05, \*\*P < 0.01, \*\*\*P < 0.001). **(K, L)** The mRNA and protein expression of HPCAL1 in HSCs after 48 h of coculture with liver macrophages. Student's t test was used for statistical analysis (\*P < 0.05). **(M)** The mRNA expression level of HPCAL1 in HSCs supplemented with exosomes secreted by control liver macrophages and activated liver macrophages after LPS treatment for 12 h. Student's t test was used for statistical analysis (\*\*P < 0.01)

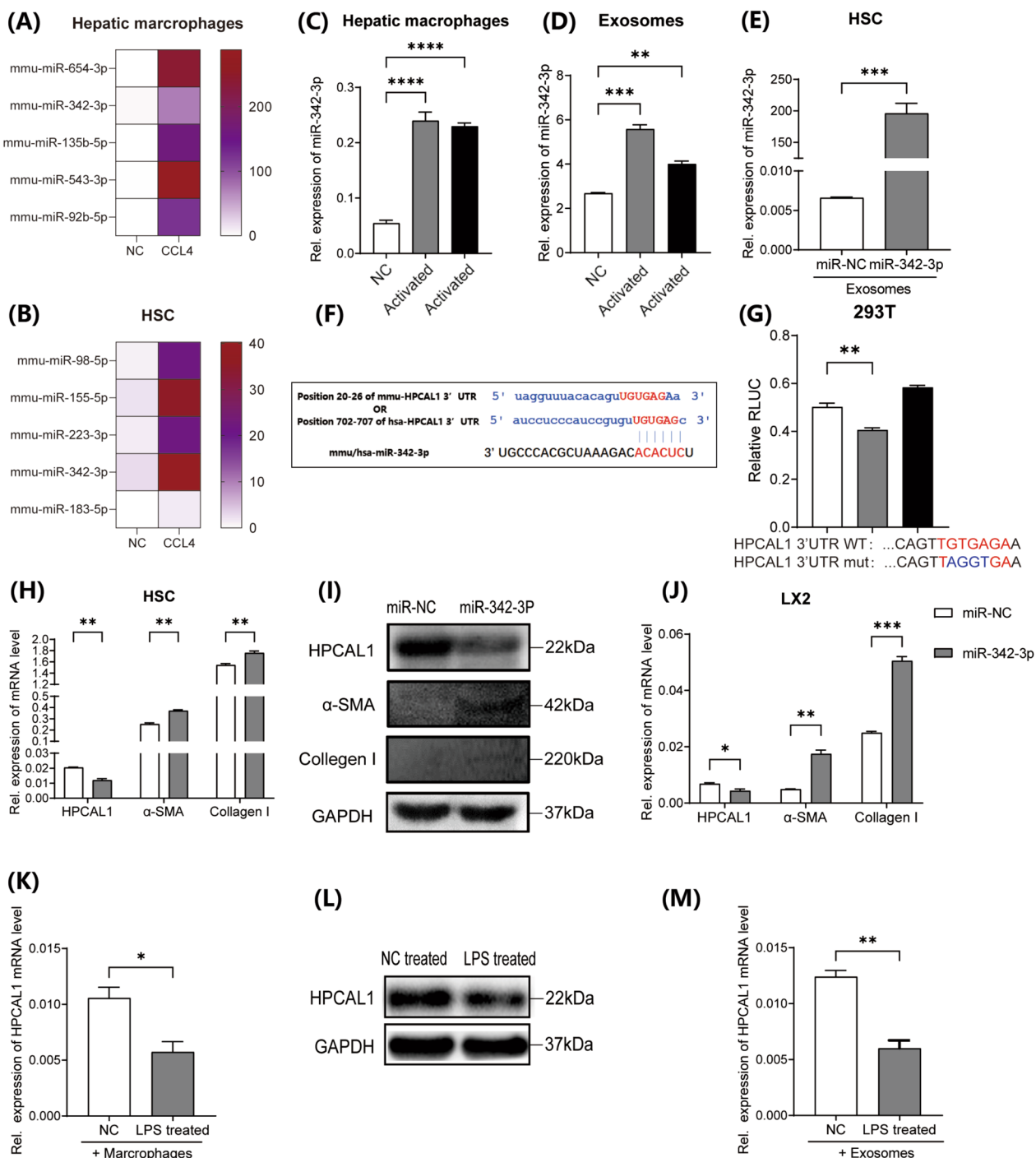


**Fig. 2** (See legend on previous page.)

with a mean particle diameter of 50–150 nm, indicating that they were exosomes derived from macrophages (Fig. 1C–E). Furthermore, we labeled the exosomes taken up by HSCs with the fluorescent dye PKH67 (Fig. 1F) and confirmed the expression of the exosome markers

CD63 and TSG101 in macrophage-derived exosomes (Fig. 1G). We then extracted exosomes from primary liver macrophages with and without LPS treatment and added them to the culture medium of primary HSCs. As expected, we observed the activation of HSCs, as

evidenced by elevated transcriptional levels of  $\alpha$ -SMA and collagen I in the LPS-treated group (Fig. 1H). Taken together, these findings suggest that exosomes can be transferred from macrophages to HSCs and play a key role in the increase in HSC activation by macrophages.

#### Macrophage-derived exosomal miRNA-342-3p promotes HSC activation by inhibiting HPCAL1

We then created an *in vivo* liver fibrosis model using CCl<sub>4</sub> and extracted exosomes from the primary macrophages of control C57B/6 J mice and C57B/6 J mice with CCl<sub>4</sub>-induced liver fibrosis. Next, we performed miRNA sequencing to identify candidate miRNAs involved in liver fibrosis. The results showed that miR-342-3p was significantly upregulated in exosomes from primary macrophages in the liver fibrosis mouse model (Fig. 2A). We also sequenced miRNAs in primary HSCs extracted from control and CCl<sub>4</sub>-induced liver fibrosis C57B/6 J mice and found that the level of miR-342-3p in primary HSCs was significantly upregulated in the CCl<sub>4</sub> group compared to the normal control (Fig. 2B). To further investigate the role of miR-342-3p in liver macrophages, we examined the expression levels of miRNA-342-3p in control primary liver macrophages (cultured for 5 days after primary cell extraction) and activated primary liver macrophages (cultured for 2 weeks after being isolated from control mice that were activated and cultured with primary liver macrophages isolated from mice with CCl<sub>4</sub>-induced liver fibrosis). MiR-342-3p was increased in activated liver macrophages (Fig. 2C). This finding further proved that miR-342-3p in exosomes was also increased in activated liver macrophages (Fig. 2D). We then treated HSCs with exosomes derived from primary macrophages transfected with miR-342-3p mimics and found that miR-342-3p was subsequently increased in HSCs (Fig. 2E). Furthermore, we searched for the downstream gene through bioinformatics analysis and identified HPCAL1 as its target gene. Sequence alignment showed that miR-342-3p could bind to wild-type HPCAL1 in the 3'-UTR (Fig. 2F). The results indicated that miR-342-3p could bind to HPCAL1 at nucleotide positions 20–26 in mice and at nucleotide positions 702–707 in humans (Fig. 2F). To determine the role

of miR-342-3p in targeting gene expression and activity, we constructed luciferase reporters with wild-type or mutant HPCAL1 and cotransfected them with miR-342-3p overexpression plasmids into HEK 293 T cells. Overexpression of miR-342-3p significantly inhibited the luciferase activity of wild-type HPCAL1, but it had no effect on the luciferase activity of cells transfected with the mutant 3'-UTR (Fig. 2G). In primary HSCs overexpressing miRNA-342-3p, the mRNA and protein levels of  $\alpha$ -SMA and collagen I were increased, while those of HPCAL1 were decreased (Fig. 2H, I). Consistent results were obtained in the LX2 cell line (Fig. 2J). After being cocultured with macrophages, HSCs showed limited transcriptional and protein levels of HPCAL1 (Fig. 2K, L). When macrophage-derived exosomes were added, we also observed decreased mRNA levels of HPCAL1 in HSCs (Fig. 2M). Taken together, these findings revealed that macrophage-derived exosomal miRNA-342-3p downregulated HPCAL1 expression to activate HSCs.

#### HPCAL1 is downregulated in the fibrotic liver tissues of mice and humans and impairs HSC activation

In patients with cirrhosis, H&E and Masson staining of liver tissue showed severe fibrosis and increased inflammatory cell infiltration, pseudolobule formation, and collagen fiber accumulation. Moreover, the immunohistochemical staining results showed that the expression of HPCAL1 was decreased in patients with cirrhosis (Fig. 3A). Similarly, compared to control mice, CCl<sub>4</sub>-treated mice had lower HPCAL1 expression in their liver tissue (Fig. 3B). Consistently, the FPKM levels of HPCAL1 in patients with cirrhosis in the GEO dataset were significantly lower than those in healthy individuals (Fig. 3C). Real-time PCR showed that the mRNA levels of HPCAL1 were lower in cirrhotic tissues than in healthy tissues (Fig. 3D). Additionally, a negative correlation was found between the RNA expression levels of  $\alpha$ -SMA and HPCAL1 in the GSE14323 dataset ( $p=0.002$ ,  $r=-0.341$ , Fig. 3E).

To verify the function of HPCAL1 in liver fibrosis, we designed lentiviruses to knock down and overexpress HPCAL1 in the LX2 cell line. Overexpression of HPCAL1 decreased the transcription of activated

(See figure on next page.)

**Fig. 3** HPCAL1 is downregulated in the fibrotic liver tissues of mice and humans. **(A)** H&E, Masson and immunohistochemical analysis of HPCAL1 expression levels in normal human liver tissues and human liver fibrotic tissues. Scale bar, 200  $\mu$ m, 10 $\times$ ; Scale bar, 100  $\mu$ m, 20 $\times$ . **(B)** immunohistochemical analysis of HPCAL1 protein in control C57Bl6 mice and a CCl<sub>4</sub>-induced liver fibrosis mouse model (8 weeks old). Scale bar, 200  $\mu$ m, 10 $\times$ ; Scale bar, 100  $\mu$ m, 20 $\times$ . **(C)** The mRNA expression levels of HPCAL1 in 19 normal liver tissues and 58 liver cirrhosis tissues in the GSE14323 database. Student's t test was used for statistical analysis (\*\* $P < 0.01$ ). **(D)** The mRNA expression levels of HPCAL1 in 14 normal liver tissues and 41 liver cirrhosis tissues in our own samples. Student's t test was used for statistical analysis (\*\* $P < 0.01$ ). **(E)** The levels of  $\alpha$ -SMA and HPCAL1 were negatively correlated in the GSE14323 dataset

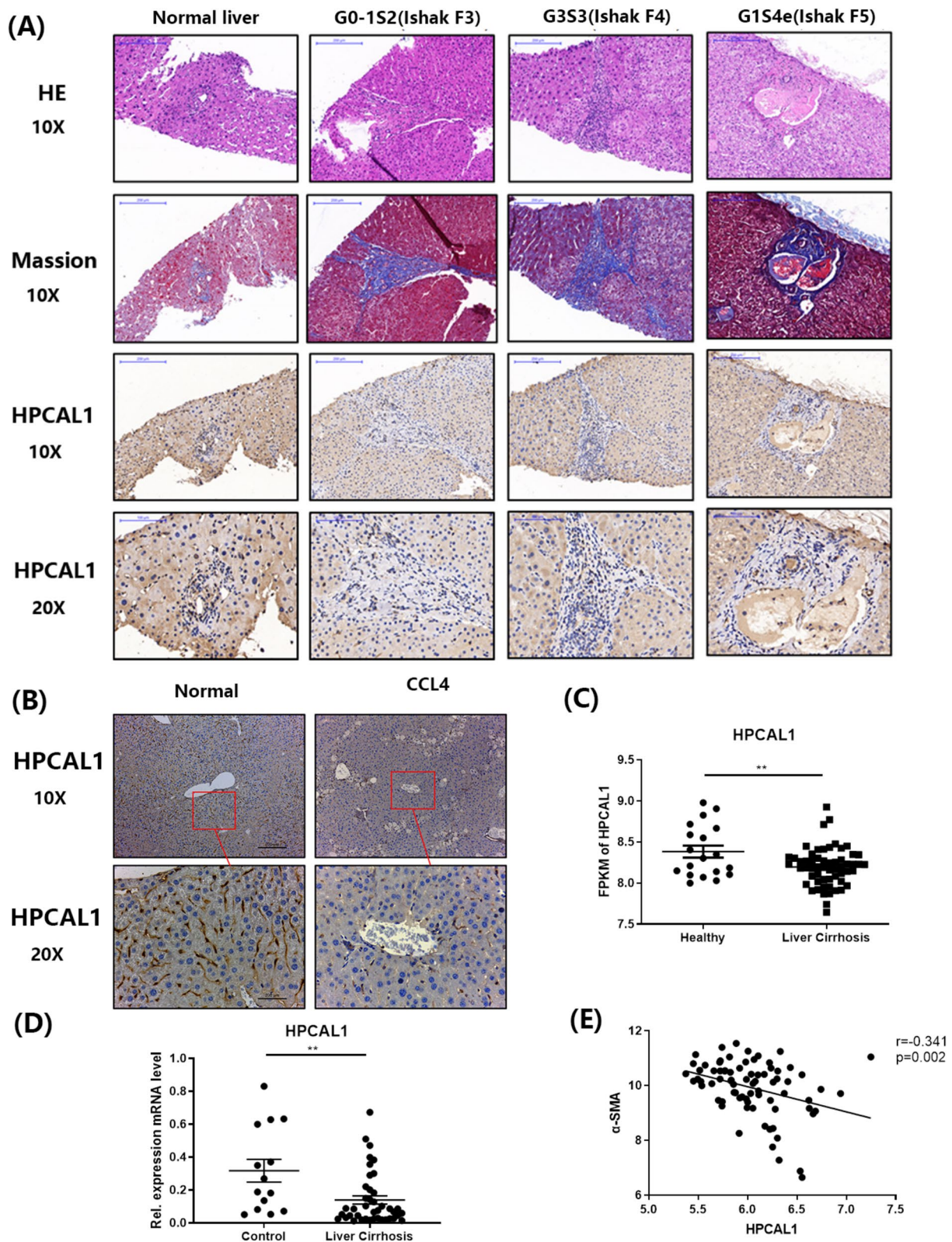


**Fig. 3** (See legend on previous page.)

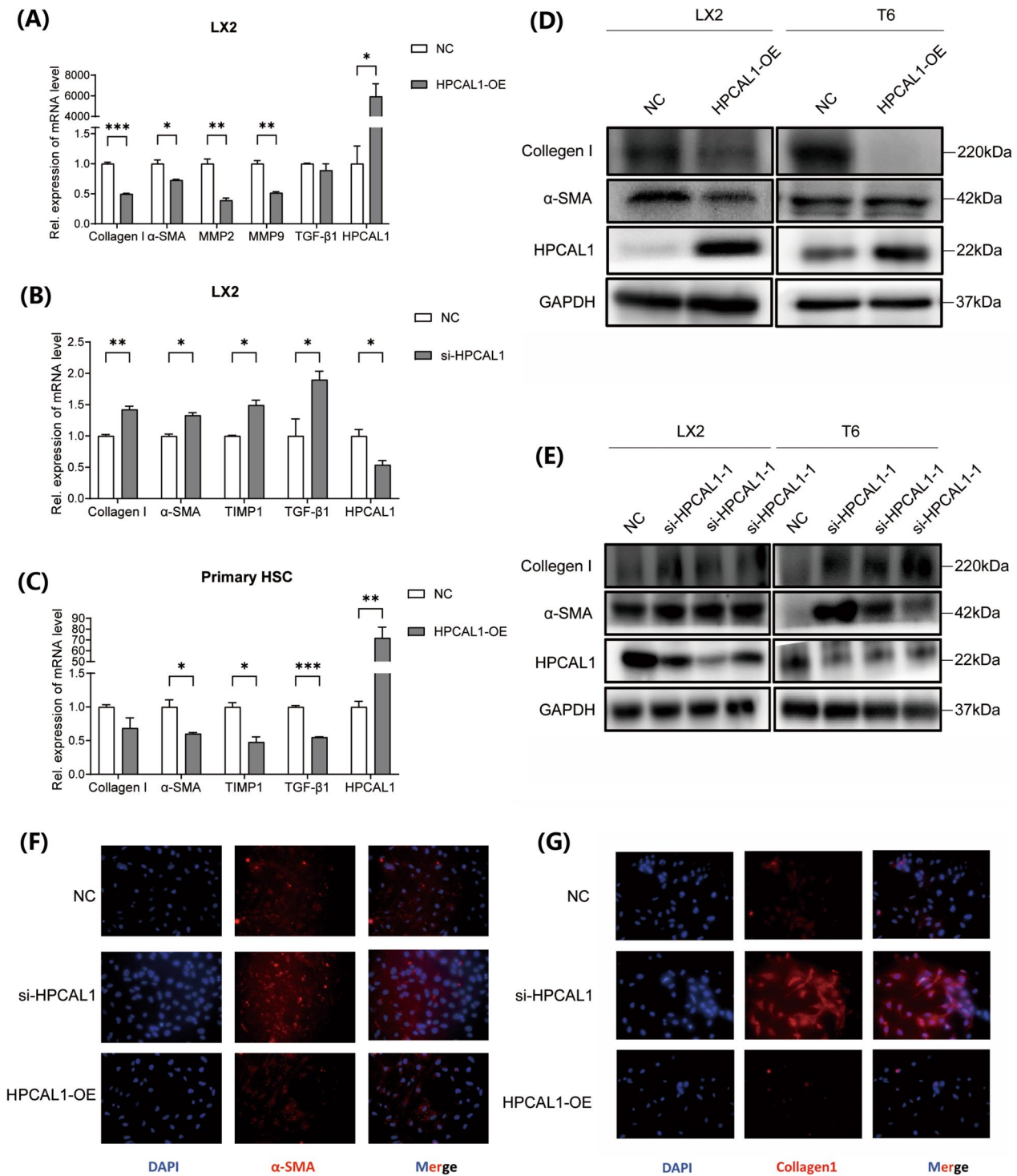


**Fig. 4** HPCAL1 suppresses HSC activation. **(A, B)** Real-time qPCR analysis of the mRNA levels of  $\alpha$ -SMA, collagen I, TIMP1, MMP2/9, TGF- $\beta$ 1 and HPCAL1 after transfection with HPCAL1 overexpression plasmids (A) or siRNA (B) in LX2 cells. **(C)** Real-time qPCR analysis of the mRNA levels of  $\alpha$ -SMA, collagen I, TIMP1, TGF- $\beta$ 1 and HPCAL1 after HPCAL1 overexpression in primary HSCs. Student's t test was used for statistical analysis (\* $P < 0.05$ , \*\* $P < 0.01$ , \*\*\* $P < 0.001$ , \*\*\*\* $P < 0.0001$ ). **(D, E)** Western blot analysis of the expression levels of  $\alpha$ -SMA and collagen I in LX2 and HSC-T6 cells after overexpressing (D) or silencing (E) HPCAL1. **(F, G)** Immunofluorescence staining was used to measure the expression of collagen I (f) and  $\alpha$ -SMA (g) after overexpressing or silencing HPCAL1 in LX2 cells. Scale bar, 50  $\mu$ m

HSC markers such as collagen I,  $\alpha$ -SMA, MMP2 and MMP9 (Fig. 4A). In contrast, si-HPCAL1 increased the levels of HSC activation-related markers in LX2 cells including collagen I,  $\alpha$ -SMA, MMP1 and TGF- $\beta$ 1 (Fig. 4B). Consistent results were also obtained in primary HSCs overexpressing HPCAL1 (Fig. 4C). Western blot and immunofluorescence analyses revealed similar changes in the protein levels of collagen I and  $\alpha$ -SMA by the regulation of HPCAL1 in LX2 and HSC-T6 cells (Fig. 4D–G). These results showed that HPCAL1 was downregulated in liver tissues from CCl<sub>4</sub>-treated mice and patients with cirrhosis and was involved in the increase in HSC activation, indicating the role of HPCAL1 as a biomarker for liver cirrhosis.

#### **HPCAL1 alleviates liver fibrosis in vivo**

In this study, the inhibitory effect of HPCAL1 on liver fibrosis was investigated in vivo. Lentiviruses overexpressing control and HPCAL1 were injected into the tail veins of mice that were treated with CCl<sub>4</sub> for 8 weeks and 12 weeks (Fig. 5D). H&E and Masson's trichrome staining showed that inflammatory infiltration and hepatic collagen deposition were significantly decreased by HPCAL1 overexpression. Immunohistochemical staining for  $\alpha$ -SMA and collagen I revealed low levels of HSC activation and extracellular collagen deposition in the livers of the mice injected with LV-HPCAL1 (Fig. 5A, B). Western blot analysis of  $\alpha$ -SMA also showed a significant decrease in mice with liver fibrosis overexpressing LV-HPCAL1 (Fig. 5C). These findings suggest that HPCAL1 overexpression gene therapy can reverse liver fibrosis.

#### **HPCAL1 inhibits TGF- $\beta$ signaling in liver stellate cells by regulating the ubiquitination of Smad2**

TGF- $\beta$ 1 plays a crucial role in HSC activation, fibrosis, and collagen accumulation during physiological repair. To better understand how HPCAL1 inhibits fibrogenesis, we investigated the TGF- $\beta$ 1 signaling pathway. After treatment of LX2 cells overexpressing HPCAL1 with TGF- $\beta$ 1, the expression of HPCAL1 was inhibited. The overexpression of HPCAL1 inhibited the expression of Smad2/Smad3 and reversed the increase in pSmad2/pSmad3 induced by TGF- $\beta$ 1 (Fig. 6A). These results

suggest that HPCAL1 can inhibit TGF- $\beta$  signaling in liver stellate cells. Additionally, we found that upregulating HPCAL1 inhibited the mRNA expression of  $\alpha$ -SMA, collagen I, and TIMP1 in TGF- $\beta$ 1-treated LX2 cells (Fig. 6B–D). We investigated the molecular mechanism by which HPCAL1 regulates Smad expression and determined that they were colocalized. In the co-IP experiment, we found that HPCAL1 could interact with Smad2/3, pSmad2/3, and Smad4 proteins (Fig. 6E), indicating that HPCAL1 directly binds with the Smad protein complex. Next, to determine which protein HPCAL1 directly binds to, we constructed the smad2/3/4 plasmid, transfected LX2 cells overexpressing HPCAL1, and performed co-IP analysis. HPCAL1 directly interacted with the Smad2 protein (Fig. 6F–H). Confocal experiments showed that HPCAL1 and Smad2 colocalized in LX2 cells (Fig. 6I) and human liver tissue (Fig. 6J). Then, 293 T cells were cotransfected with HPCAL1 and Smad2 expression plasmids and the ubiquitin-labeled plasmid HA for 48 h and treated with the proteasome inhibitor MG132 (10  $\mu$ M) for 24 h. Coimmunoprecipitation was performed with lysates treated with anti-Smad2 mAb-magnetic beads. The level of ubiquitination in the HPCAL1 overexpression group was increased, suggesting that HPCAL1 promoted Smad2 degradation through proteasome ubiquitination (Fig. 6K). Moreover, the EF-hand 4 domain of HPCAL1 mediated the association with Smad2 (Fig. 6L, M). Overall, our findings suggest that HPCAL1 inhibits fibrogenesis in liver stellate cells by directly interacting with Smad2 and promoting its degradation through proteasome ubiquitination. These results provide a therapeutic target for the treatment of liver fibrosis.

#### **Discussion**

Liver fibrosis results from damage to hepatocytes and cholangiocytes, which activates innate immune responses, macrophages and HSCs [19]. The activation of innate immune responses in the liver, including neutrophils, macrophages, natural killer (NK) cells, NKT cells, innate lymphoid cells, B cells, and T cells, follows the activation of DAMPs and PAMPs, further contributing to liver injury and fibrosis progression [9, 20, 21]. HSCs are persistently activated and produce and accumulate ECM.

(See figure on next page.)

**Fig. 5** HPCAL1 alleviates liver fibrosis in vivo. **(A)** H&E staining and immunohistochemical analysis of Masson's trichrome staining and the expression of  $\alpha$ -SMA and collagen I in control C57/B mice, mice with CCl<sub>4</sub>-induced liver fibrosis at 8-weeks and 12-weeks, and mice with LV-HPCAL1 overexpression after an intravenous injection (n = 5 mice). Scale bar, 50  $\mu$ m. **(B)** Data are presented as the mean  $\pm$  SEM (n = 5). Student's t test was used for statistical analysis (\*P < 0.05, \*\*P < 0.01, \*\*\*P < 0.001, \*\*\*\*P < 0.0001). **(C)** Western blot analysis of  $\alpha$ -SMA in control C57BL/6 mice, mice with CCl<sub>4</sub>-induced liver fibrosis at 8-weeks and 12-weeks, and mice overexpressing LV-HPCAL1 by intravenous injection (n = 5 mice). **(D)** Real-time qPCR analysis of the mRNA levels of HPCAL1 in the livers of control C57BL mice, mice with CCl<sub>4</sub>-induced liver fibrosis at 8-weeks and 12-weeks, and mice overexpressing LV-HPCAL1 by intravenous injection (n = 5 mice). Student's t test was used for statistical analysis (\*\*P < 0.01)

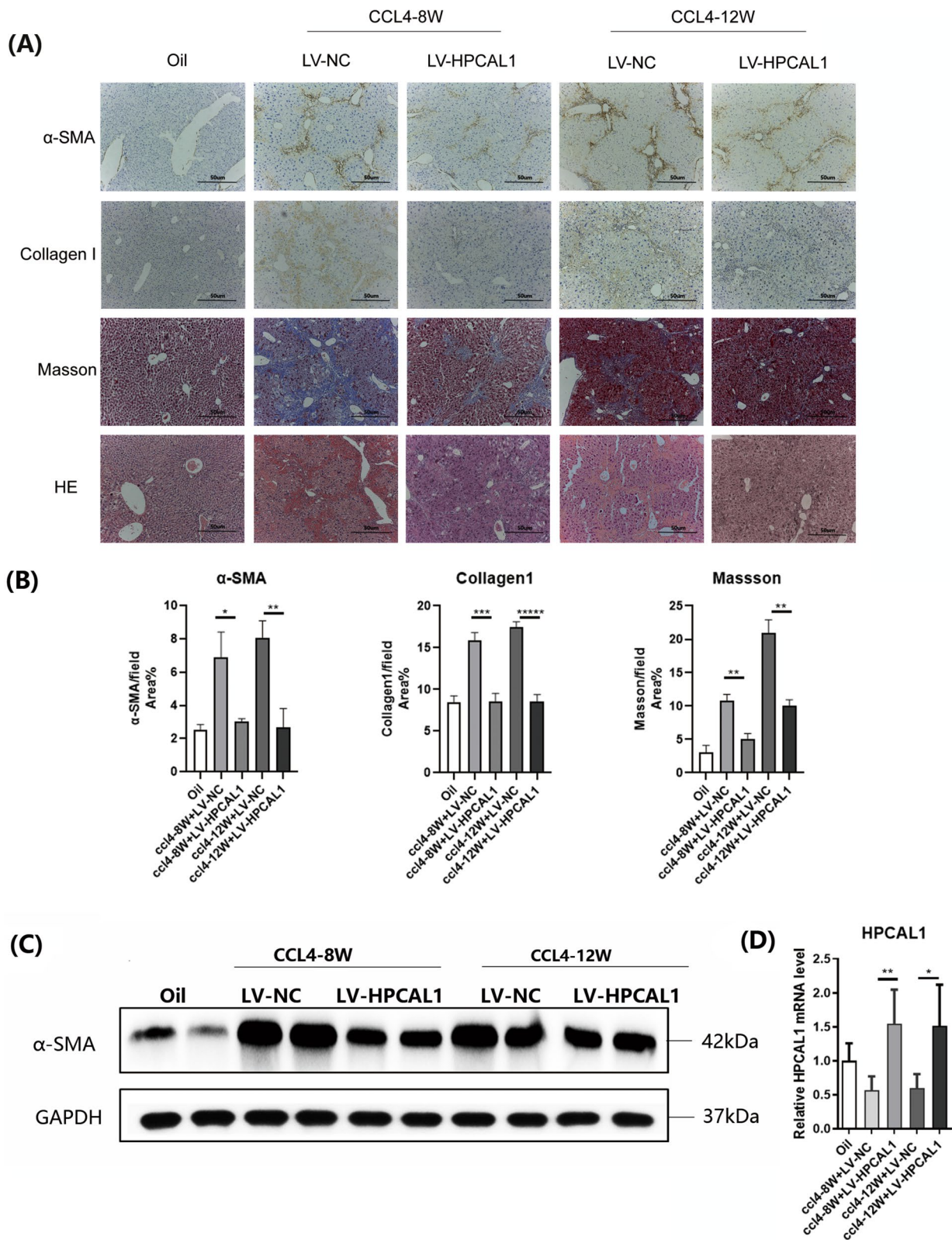


**Fig. 5** (See legend on previous page.)

TGF- $\beta$  plays a vital role in the activation of HSCs by activating the SMAD2/3/4 complex and transcriptionally upregulating  $\alpha$ -SMA and collagen I expression. Smad2 ubiquitination plays a key role in regulating TGF- $\beta$  signaling by controlling Smad2 stability. When Smad2 is ubiquitinated, it is marked for proteasomal degradation, reducing the duration and intensity of TGF- $\beta$  signaling. Enhanced Smad2 ubiquitination accelerates its degradation, preventing excessive TGF- $\beta$  signaling and the activation of fibrogenic pathways. E3 ubiquitin ligases like Smurf1 and WWP1 are involved in regulating Smad2 ubiquitination, and disrupting this process can worsen fibrosis by enhancing TGF- $\beta$  signaling. Exosomes, which transfer cargo materials such as proteins or nucleic acids, play a vital role in intercellular communication and can alter the biological behaviors of recipient cells. These vesicles exhibit flexible characteristics, and orchestrate liver health and disease and play a vital role in the diagnosis and treatment of liver diseases [22]. Additionally, miR-500 overexpression in macrophage exosomes could significantly promote HSC proliferation and activation [11].

Our study first showed that hepatic macrophages could affect the activation of stellate cells by secreting exosomes containing microRNA-342-3p. It has been reported that recruited BMDMs are a key component of acute and chronic liver injury and inflammation involved in the regression of liver disease [23, 24]. Moreover, it was found that the miR-342-3p expression level gradually increased on the 3rd, 5th and 7th days after BMDM differentiation, suggesting that miR-342-3p expression was gradually upregulated during macrophage activation. In addition, miR-342-3p can promote M2 cell apoptosis when macrophages are polarized to the M2 phenotype after being regulated by IL-4. M2 macrophages help to eliminate inflammation and have the opposite effect as proinflammatory macrophages. These results suggest that miR-342-3p is important in macrophage activation [25, 26]. To investigate this further, we extracted primary liver macrophages from control mice and mice

with CCl<sub>4</sub>-induced liver fibrosis. After measuring the level of miR-342-3p, we found that the expression of miR-342-3p was upregulated in liver macrophages from mice with liver fibrosis. However, off-target effects are a common challenge in miRNA research, as miRNAs can bind to sequences with partial complementarity to their intended targets, leading to the regulation of additional genes beyond the primary target. These off-target effects often arise from imperfect seed matches, where miRNA sequences partially align with other mRNA regions, causing unintended silencing. Therefore, miR-342-3p may not be the sole regulator of HPCAL1 expression. A network of miRNAs likely collaborates to fine-tune HPCAL1 regulation. In brief, our results solidly demonstrate that miR-342-3p directly regulates HPCAL1 and is contained in exosomes secreted by liver macrophages, influencing HSC activation. The altered levels of miR-342-3p in exosomes can promote HSC proliferation and activation through targeting HPCAL1. This highlights the critical role of miR-342-3p in the communication between liver macrophages and HSCs.

HPCAL1 has been reported to be mainly expressed in Purkinje cells in the cerebellum. This protein belongs to the vertebrae-like protein (VILIP) superfamily, which also includes VILIP1, VILIP2, VILIP3 (gene name HPACA1), hippocalcin and neuroalcalin-D. These members have four EF-hand calcium domains and a consistent myristoylation site at the NH end. HPCAL1 can undergo conformational changes induced by calcium ions, and three Ca<sup>2+</sup> ions are synergistically bound with VILIP-3 at EF2, EF3 and EF4 (an apparent dissociation constant ( $K_d$ ) of 0.52  $\mu$ M and positive cooperativity (Hill slope = 1.8)). The existence of the EF-hand domain and the incorporation of the myristoylation sequence at the N-terminus enable VILIP-like proteins to be transported from the cytoplasm to subcellular organelle membranes, especially when the calcium ion level in the cytoplasm increases [13, 16, 27]. HPCAL1 plays a significant role in the formation and development of tumors. For instance, HPCAL1 promotes

(See figure on next page.)

**Fig. 6** HPCAL1 inhibits TGF- $\beta$  signaling in liver stellate cells by regulating the ubiquitination of Smad2. **(A)** HPCAL1 significantly inhibited the expression of Smad2/3 and pSmad2/3 in LX2 cells treated with TGF- $\beta$ 1 compared with control LX2 cells. **(B-D)** Real-time qPCR analysis of the mRNA levels of  $\alpha$ -SMA (B), collagen I (C) and TIMP1 (D) in TGF- $\beta$ 1-treated control LX2 cells and LX2 cells overexpressing HPCAL1. **(E)** In LX2 control and HPCAL1-overexpressing cells, a coimmunoprecipitation assay was used to show that HPCAL1 could interact with Smad2, Smad3, pSmad2, pSmad3 and Smad4 proteins. **(F-H)** A coimmunoprecipitation assay was used to show that Smad2 (F) could interact with HPCAL1 but not Smad3 (G) or Smad4 (H) after LX2 cells overexpressed HPCAL1 and Smad2, Smad3 or Smad4. **(I)** Immunofluorescence assay showing the colocalization of HPCAL1 and Smad2 in LX2 cells with HPCAL1 overexpression or silencing. **(J)** Immunofluorescence assay showing the colocalization of HPCAL1 and Smad2 in human liver fibrosis tissues and normal human liver tissues. **(K)** 293 T cells were divided into three groups: overexpression NC, overexpression of Smad2 and HA-Ubb, and overexpression of Smad2, HPCAL1 and HA-Ubb. Then, the cells were treated with MG132 (final concentration of 10  $\mu$ M) for 24 h. Immunoprecipitation was performed with Smad2 antibodies. **(L, M)** Flag-labeled HPCAL1 EF-hand 4 motif and Smad2 were overexpressed in 293 T cells, and immunoprecipitation was performed with Smad2 antibodies, suggesting that Smad2 binds directly to the EF4 motif of HPCAL1

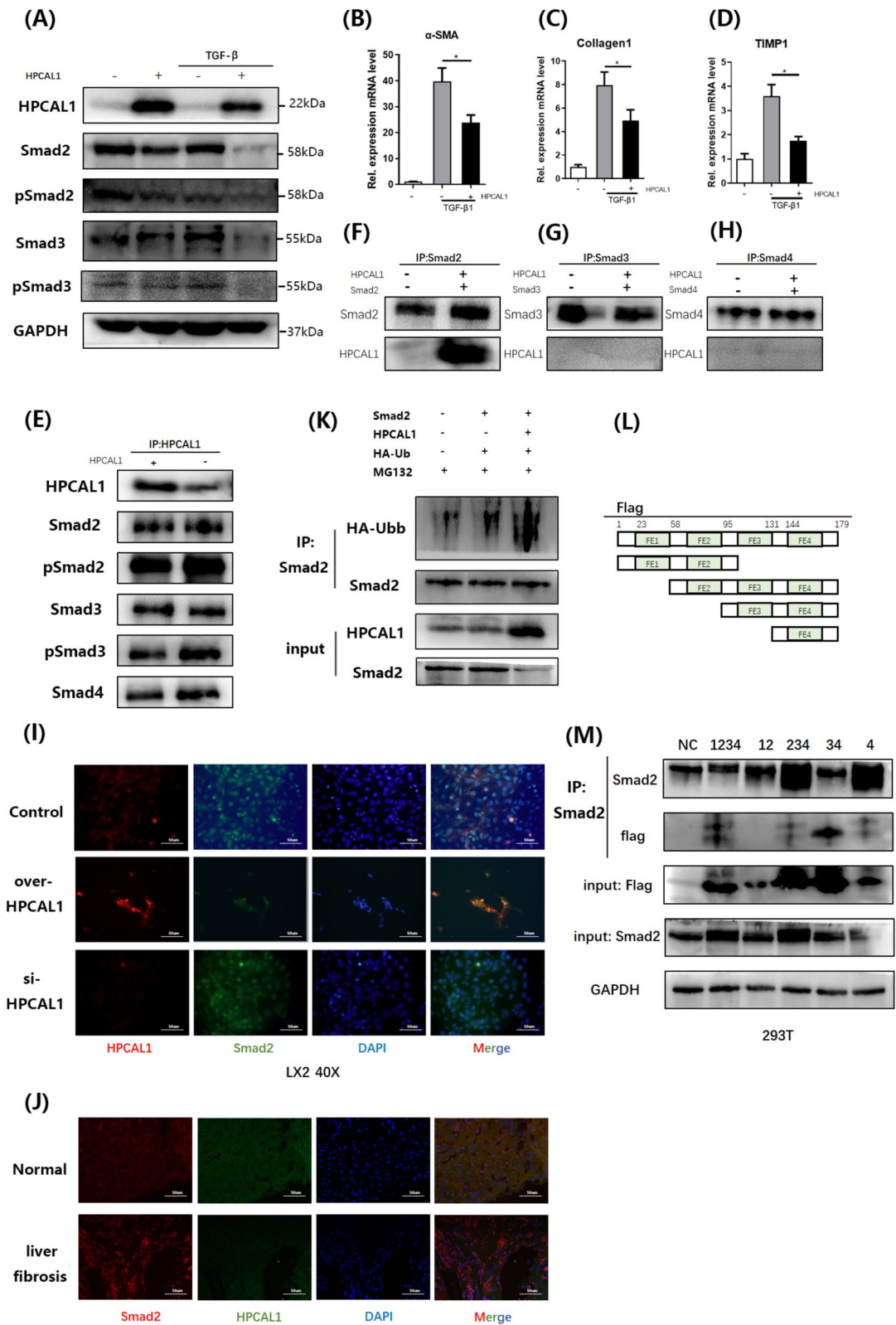


Fig. 6 (See legend on previous page.)

tumor growth by activating the WNT-CTNNB1/ $\beta$ -catenin (catenin beta 1) pathway [13]. HPCAL1 has been shown to act as a novel tumor suppressor that regulates cell cycle progression upstream of the effector protein p21 [16]. Thus, it may serve as a diagnostic and prognostic factor for HCC therapy. High expression of HPCAL1 could be a poor prognostic factor of cholangiocarcinoma but promotes the growth of non-small cell lung carcinoma [12, 15].

Liver fibrosis, which is a precancerous lesion of HCC, plays an important role in clinical outcomes. Fibrosis is also a key aspect of irreversible and potentially life-threatening liver injury, and it is a significant research topic. Our study showed that treating a mouse model of liver fibrosis induced by CCl<sub>4</sub> with a tail vein injection of lentivirus overexpressing HPCAL1 could alleviate liver fibrosis, indicating that HPCAL1 can inhibit the progression of liver fibrosis. It has been demonstrated that inhibiting TGF- $\beta$ -Smad signaling reduces the accumulation of ECM in fibrosis [28–30]. Our findings showed that HPCAL1 inhibited TGF- $\beta$  signaling in liver stellate cells by regulating the ubiquitination of Smad2 by directly interacting with the EF-hand 4 domain of HPCAL1. However, there are several limitations to our study. First, the long-term effects and potential side effects of HPCAL1 overexpression on liver function remain unclear and require further investigation. Second, the precise molecular mechanisms by which HPCAL1 regulates ECM accumulation and fibrosis progression in other cell types need to be elucidated. Despite these limitations, targeting HPCAL1 holds significant promise for the treatment of fibroproliferative liver diseases.

## Conclusions

In conclusion, our findings suggest a new profibrotic mechanism for crosstalk between macrophages and HSCs in the liver, and also highlight an attractive therapeutic strategy for treating fibroproliferative liver diseases.

## Abbreviations

HSC	Hepatic stellate cell
HPCAL1	Hippocalcin-like protein 1
HCC	Hepatocellular carcinoma
ECM	Extracellular matrix
BMDM	Bone marrow-derived macrophage
LPS	Lipopolysaccharide
VILIP	Visinin-like protein
cDNA	Complementary DNA
BSA	Bovine serum albumin
DAPI	4,6-Diamino-2-phenyl indole
EP	Eppendorf
IRB	Institutional Review Board
$\alpha$ -SMA	Alpha-smooth muscle actin
collagen I	Collagen type I
CCl <sub>4</sub>	Carbon tetrachloride
NK	Natural killer

## Author contributions

Conceptualization: WSL and JZ; Methodology: WSL; Formal Analysis: WSL; Data Curation: QZ and WWZ; Writing—Original Draft Preparation: WSL, LRC and QZ; Writing—Review & Editing: WSL and JZ; Supervision: TSH, ZGL and JL; Funding Acquisition: WSL. All authors read and approved the final manuscript.

## Funding

This work was sponsored by Shanghai Sailing Program (No.20YF1404200) and supported by National Natural Science Foundation of China (Project 82100659).

## Availability of data and materials

No datasets were generated or analysed during the current study.

## Declarations

### Ethics approval and consent to participate

All animal experiments were approved by the Ethics Committee of Huashan Hospital, Fudan University, China (No. 2021JS-395). All human liver tissue studies were approved by the Ethics Committee of Huashan Hospital, Fudan University, China (No. 2022-958). The experiments were undertaken with the understanding and written consent of each subject.

### Consent for publication

All human participants have consented to publication.

### Competing interests

The authors declare no competing interests.

### Author details

<sup>1</sup>Department of Digestive Diseases, Huashan Hospital, Fudan University, Shanghai 200040, China. <sup>2</sup>Department of Digestive Diseases, Shanghai Guanghua Hospital of Integrated Traditional Chinese And Western Medicine, Shanghai 200040, China.

Received: 13 April 2024 Accepted: 20 January 2025

Published online: 05 February 2025

## References

1. Tsochatzis EA, Bosch J, Burroughs AK. Liver cirrhosis. *Lancet*. 2014;383(9930):1749–61.
2. Kalluri R, LeBleu VS. The biology, function, and biomedical applications of exosomes. *Science* 2020;367(6478):eaau6977.
3. Campana L, Esser H, Huch M, Forbes S. Liver regeneration and inflammation: from fundamental science to clinical applications. *Nat Rev Mol Cell Biol*. 2021;22(9):608–24.
4. Kisseleva T, Brenner D. Molecular and cellular mechanisms of liver fibrosis and its regression. *Nat Rev Gastroenterol Hepatol*. 2021;18(3):151–66.
5. Heymann F, Tacke F. Immunology in the liver—from homeostasis to disease. *Nat Rev Gastroenterol Hepatol*. 2016;13(2):88–110.
6. Krenkel O, Tacke F. Liver macrophages in tissue homeostasis and disease. *Nat Rev Immunol*. 2017;17(5):306–21.
7. Marques PE, Amaral SS, Pires DA, et al. Chemokines and mitochondrial products activate neutrophils to amplify organ injury during mouse acute liver failure. *Hepatology*. 2012;56(5):1971–82.
8. Gao B, Radaeva S, Park O. Liver natural killer and natural killer T cells: immunobiology and emerging roles in liver diseases. *J Leukoc Biol*. 2009;86(3):513–28.
9. Shen M, Shen Y, Fan X, Men R, Ye T, Yang L. Roles of macrophages and exosomes in liver diseases. *Front Med (Lausanne)*. 2020;7: 583691.
10. Hirsova P, Ibrahim SH, Krishnan A, et al. Lipid-induced signaling causes release of inflammatory extracellular vesicles from hepatocytes. *Gastroenterology*. 2016;150(4):956–67.
11. Chen L, Huang Y, Duan Z, et al. Exosomal miR-500 derived from lipopoly-saccharide-treated macrophage accelerates liver fibrosis by suppressing MFN2. *Front Cell Dev Biol*. 2021;9: 716209.

12. Wang X, Xie X, Zhang Y, et al. Hippocalcin-like 1 is a key regulator of LDHA activation that promotes the growth of non-small cell lung carcinoma. *Cell Oncol (Dordr)*. 2022;45(1):179–91.
13. Zhang D, Liu X, Xu X, et al. HPCAL1 promotes glioblastoma proliferation via activation of Wnt/ $\beta$ -catenin signalling pathway. *J Cell Mol Med*. 2019;23(5):3108–17.
14. Ma M, Zeng G, Li J, et al. Expressional and prognostic value of HPCAL1 in cholangiocarcinoma via integrated bioinformatics analyses and experiments. *Cancer Med*. 2023;12(1):824–36.
15. Ma M, Zeng G, Li J, et al. Expressional and prognostic value of HPCAL1 in cholangiocarcinoma via integrated bioinformatics analyses and experiments. *Cancer Med*. 2022
16. Zhang Y, Liu Y, Duan J, et al. Hippocalcin-like 1 suppresses hepatocellular carcinoma progression by promoting p21(Waf/Cip1) stabilization by activating the ERK1/2-MAPK pathway. *Hepatology*. 2016;63(3):880–97.
17. Chen X, Song X, Li J, et al. Identification of HPCAL1 as a specific autophagy receptor involved in ferroptosis. *Autophagy* 2022;1–21.
18. Zhu J, Luo Z, Pan Y, et al. H19/miR-148a/USP4 axis facilitates liver fibrosis by enhancing TGF- $\beta$  signaling in both hepatic stellate cells and hepatocytes. *J Cell Physiol*. 2019;234(6):9698–710.
19. Koyama Y, Brenner DA. Liver inflammation and fibrosis. *J Clin Invest*. 2017;127(1):55–64.
20. Tacke F, Zimmermann HW. Macrophage heterogeneity in liver injury and fibrosis. *J Hepatol*. 2014;60(5):1090–6.
21. Matsuda M, Seki E. Hepatic stellate cell-macrophage crosstalk in liver fibrosis and carcinogenesis. *Semin Liver Dis*. 2020;40(3):307–20.
22. Chen L, Yao X, Yao H, Ji Q, Ding G, Liu X. Exosomal miR-103-3p from LPS-activated THP-1 macrophage contributes to the activation of hepatic stellate cells. *FASEB J*. 2020;34(4):5178–92.
23. Starkey Lewis P, Campana L, Aleksieva N, et al. Alternatively activated macrophages promote resolution of necrosis following acute liver injury. *J Hepatol*. 2020;73(2):349–60.
24. Liu K, Zhao E, Ilyas G, et al. Impaired macrophage autophagy increases the immune response in obese mice by promoting proinflammatory macrophage polarization. *Autophagy*. 2015;11(2):271–84.
25. Self-Fordham JB, Naqvi AR, Uttamani JR, Kulkarni V, Nares S. MicroRNA: Dynamic Regulators of Macrophage Polarization and Plasticity. *Front Immunol (Internet)* 2017 (cited 2019 Mar 13);8. <https://doi.org/10.3389/fimmu.2017.01062/full#B83>
26. Yuanyuan W, Maliheh N-J, Lily C, et al. The microRNA-342-5p fosters inflammatory macrophage activation through an Akt1- and microRNA-155-dependent pathway during atherosclerosis. *Circulation*. 2013;127(15):1609–19.
27. Chen X, Song X, Li J, et al. Identification of HPCAL1 as a specific autophagy receptor involved in ferroptosis. *Autophagy*. 2023;19(1):54–74.
28. Marra F, Tacke F. Roles for chemokines in liver disease. *Gastroenterology*. 2014;147(3):577–594.e1.
29. Shrestha N, Chand L, Han MK, Lee SO, Kim CY, Jeong YJ. Glutamine inhibits CCl4 induced liver fibrosis in mice and TGF- $\beta$ 1 mediated epithelial-mesenchymal transition in mouse hepatocytes. *Food Chem Toxicol*. 2016;93:129–37.
30. Kumar S, Duan Q, Wu R, Harris EN, Su Q. Pathophysiological communication between hepatocytes and non-parenchymal cells in liver injury from NAFLD to liver fibrosis. *Adv Drug Deliv Rev*. 2021;176: 113869.

## Publisher's Note

Springer Nature remains neutral with regard to jurisdictional claims in published maps and institutional affiliations.